Kinetic analysis of the interaction between amphotericin B and human serum albumin using surface plasmon resonance and fluorescence spectroscopy

Bo Zhou, Ran Li, Yue Zhang and Yi Liu*

Received 19th November 2007, Accepted 11th February 2008
First published as an Advance Article on the web 21st February 2008
DOI: 10.1039/b717897b

The binding interaction between amphotericin B and human serum albumin (HSA) has been studied using surface plasmon resonance (SPR) spectroscopy combined with a fluorescence quenching method to confirm the binding kinetic results. In this paper, the SPR method used to study the drug–protein interaction has been described in detail. The association rate constant, dissociation rate constant and the equilibrium association constant of amphotericin B binding to HSA were obtained using this method. To confirm the feasibility of the SPR method, a fluorescence quenching method was performed to obtain the equilibrium constant. In order to obtain more accurate results, experiment design was used to optimize the fluorescence quenching process. The two equilibrium association constants obtained using the two methods were 4.017×10^4 M^{-1} (SPR) and 3.656×10^4 M^{-1} (fluorescence quenching method) respectively.

1 Introduction

The studies of drug–target interactions are helpful in the fields of pharmacokinetics, pharmacodynamics, and drug discovery. As the major soluble protein constituents of the circulatory system, serum albumins have many physiological functions. The albumins contribute significantly to colloid osmotic blood pressure and aid in the transport, distribution and metabolism of many endogenous and exogenous ligands.[1] Many drugs and other bioactive small molecules can bind reversibly to albumins. Binding studies are important because only the unbound drug is pharmacologically active.[2] Therefore, studying the binding between a drug and human serum albumin (HSA) can help to learn about the property of the drugs transported in blood.

Amphotericin B (AmB), a polyene antifungal agent (Fig. 1), was first isolated by Gold *et al.* from Streptomyces nodosus in 1955. For ten years, AmB has been used as the standard drug used for the treatment of systemic fungal infections due to lack of alternatives, although AmB is toxic to mammalian cells. Several researches have been performed to study the interaction between AmB and sterol, for it is generally accepted that the binding between AmB and ergosterol, the main sterol in fungal cell membranes, may lead to the death of cells.[3–7] However, as a drug, the interaction between AmB and the model transport protein HSA has not been studied before. Therefore, the mainly purpose of this study was to determine the binding parameters between AmB and HSA.

Surface plasmon resonance (SPR) is a relatively new method to monitor the molecule interactions since the first commercial instrument was introduced in 1990. It is an optical technique based on the measurement of the changes of refractive index very close to a metal (*e.g.* Au or Ag) surface. In order to detect the interaction, one molecule (the ligand) should be immobilized on the surface and the other (the analyte) is injected in aqueous solution through the flow cell. As the interaction takes place, the refractive index changes and the changes can be recorded.[8–10] The major advantage of SPR is that the interaction process can be monitored in real-time without labeling requirements. Another advantage is that both the association and dissociation rate constants can be obtained except for the equilibrium association constant. This method has been widely used in biochemical, biophysical and biomedical fields. In the past few years, many papers about SPR technology have been published.[11–17] The use of SPR sensors makes it possible to monitor the reactions of drug–protein,[1,18] DNA–protein,[19,20] antibody-microorganism,[21] protein–receptor,[22,23] low molecular substance–protein[24], antibody–antigen[25] and so on.

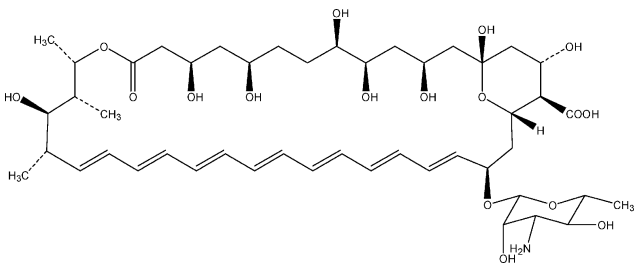

Fig. 1 The structure of amphotericin B.

Since the SPR method is a relatively new method to study binding interactions, to confirm our results, we also used a fluorescence quenching method. This is a traditional and easy to use method for monitoring binding interactions.[26] It can reveal the accessibility of quenchers to albumin's fluorophore groups, help to understand albumin's binding mechanisms to drugs, and provide clues to the nature of the binding phenomenon.[27] In this paper, this method was used to prove that our SPR method could be used to study drug–protein interactions and be more helpful in the kinetic parameter determination. In order to obtain more accurate results, experimental design[28] was used to optimize the measurement conditions of the fluorescence quenching.

State Key Laboratory of Virology, College of Chemistry and Molecular Science, Wuhan University, Wuhan 430072, P. R. China. E-mail: prof.liuyi@263.net, liuyi@chem.whu.edu.cn; Fax: +86-27-6854067; Tel: +86-27-87218284

2. Results and discussions

2.1 Characterization of the 11-MUA self-assembled monolayer

The cyclic voltammograms of the bare gold film and 11-MUA modified gold film are shown in Fig. 2 (in phosphate buffer solution) and Fig. 3 (in $K_3Fe(CN)_6$ solution). The peak current of (b) is obviously lower than (a) which proves that the gold film has been modified by 11-MUA.

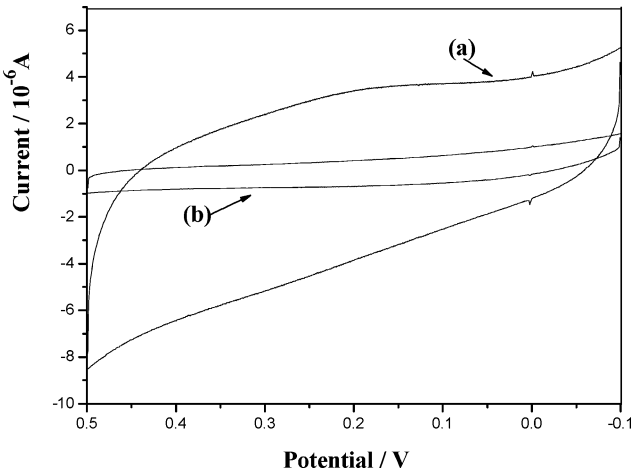

Fig. 2 Cyclic voltammograms of the bare (a) and the modified gold film (b) in PBS (pH = 7.00).

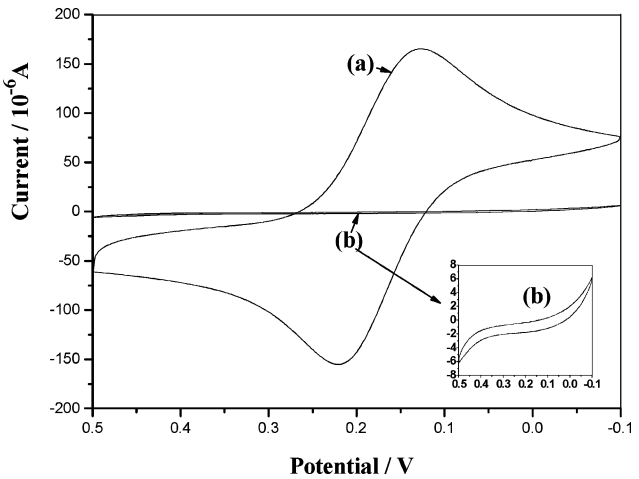

Fig. 3 Cyclic voltammograms of the bare (a) and the modified gold electrode (b) in 0.1 mM $K_3Fe(CN)_6$+0.1 M KCl.

To confirm the formation of 11-MUA self-assembled monolayer, X-ray photoelectron spectroscopy (XPS) measurements werw performed. As shown in Fig. 4, the binding energy of S 2p occurs at 162.5 eV. This indicates a Au–S bond formation with loss of a sulfhydryl hydrogen.[29,30]

During the SPR experiment process, the formation of the monolayer could also be detected. As shown in Fig. 5, after the injection of NHS–EDC, the signal of (a) (bare gold film) returns to the baseline (slight lower than original baseline), while the signal of (b) (11-MUA modified gold film) is much higher than the baseline. Therefore there must be something immobilized on film

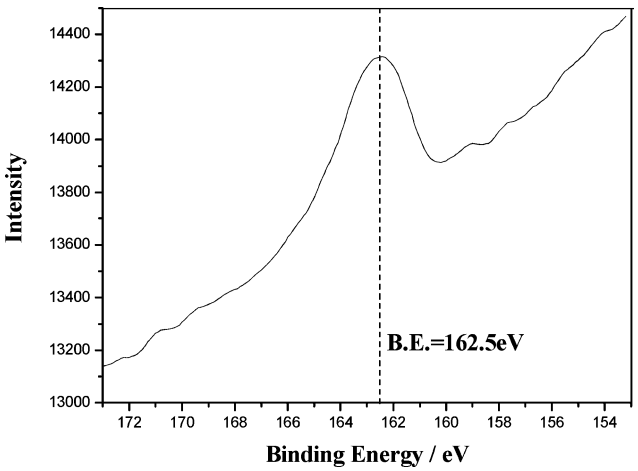

Fig. 4 The XPS spectra of Au–S bond formation.

(b) because of the interaction between NHS–EDC and carboxyl group. So we can confirm that the film was modified with 11-MUA. The signal of sample (b) drops suddenly to the bottom and returns when the injection of NHS–EDC was over, because the signal is too strong to overflow during the injection process.

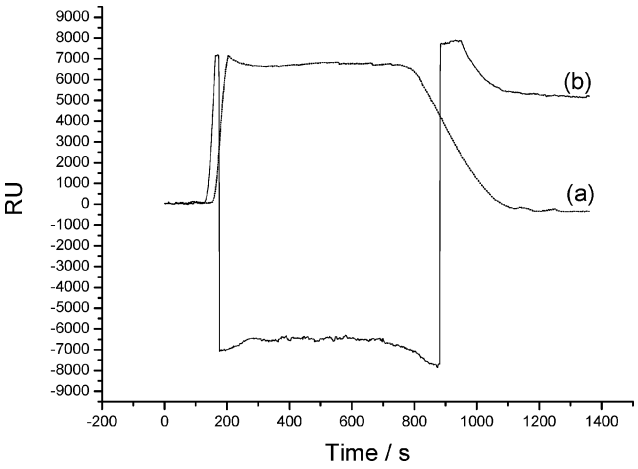

Fig. 5 The SPR signal of the injection of NHS–EDC.

2.2 Binding kinetic analysis between amphotericin B (AmB) and HSA

When AmB reacts with HSA to form a complex, the rate of the complex formation depends on the free concentration of AmB, HSA and the stability of the formed complex, which can be described by the following equation:

$$d[AmB–HSA]/dt = k_a[AmB][HSA] - k_d[AmB–HSA] \quad (1)$$

where k_a is the association rate constant and k_d is the dissociation rate constant. HSA was immobilized as the ligand and AmB was injected in the flow system as the analyte.

In the SPR biosensor, the concentration of bound AmB is proportional to the response R. The free ligand concentration [HSA] is the difference between total and bound ligand concentration. The total concentration of active immobilized HSA is obtained indirectly as it is saturated with analyte. The maximum response

due to analyte binding, R_{max}, will therefore be proportional to the total ligand concentration and ($R_{max} - R$) will be proportional to the free HSA concentration. When AmB is injected in a flow cell over the sensor surface, the AmB solution is constantly replenished and hence the free concentration of Amp may be considered constant and identical to the total AmB concentration. The reaction between immobilized HSA and AmB in solution can therefore be assumed to follow pseudo first order kinetics and since the concentration of the complex and free HSA now can be expressed in terms of AmB response, eqn (1) can be rewritten as

$$dR/dt = k_a C(R_{max} - R) - k_d R \quad (2)$$

where C is the concentration of injected AmB.

A simple rearrangement of eqn (2) gives

$$dR/dt = k_a C R_{max} - (k_a C + k_d)R \quad (3)$$

Rate constants can now be evaluated from a plot of dR/dt *vs.* R provided that R_{max} and C are known. When several concentrations of AmB are injected, the slope value k_s, obtained from each dR/dt *vs.* R plot, can be introduced into a new plot *vs.* AmB concentration with

$$k_s = k_a C + k_d \quad (4)$$

The association and the dissociation rate constant can be obtained from this relationship (Fig. 6). Then the equilibrium constant K_A can be calculated by $K_A = k_a/k_d$

In this kind of solid-based biosensors, some deviations may be caused by the surface artifacts, such as mass transport and chemical or spatial heterogeneity. Therefore, separately fitting selected portions of the association and dissociation phase data is not a satisfying approach to get accurate results. Ideally, one would like to show that the entire data set is described by a particular reaction mechanism using global analysis.[31] Here we used ClmapXP software to do the global analysis based on a simple biomolecular interaction model AmB + HSA ⇌ AmB–HSA

Fig. 7 shows the binding curves between amphotericin B and HSA. The kinetic constants of the binding interaction were calculated using ClampXP software, as shown in Table 1.

From Table 1, we can see that the high capacity surface could be obtained by injecting high concentration HSA (R_{max} is 410.0 and 264.7 for 25 μg mL^{-1}, 5 μg mL^{-1} respectively). The values of K_A of high capacity surface is bigger than that of low capacity one. However, the standard error of the high capacity surface (0.568) is bigger than the low capacity one (0.060), which could also be expressed as the deviation between the original lines and

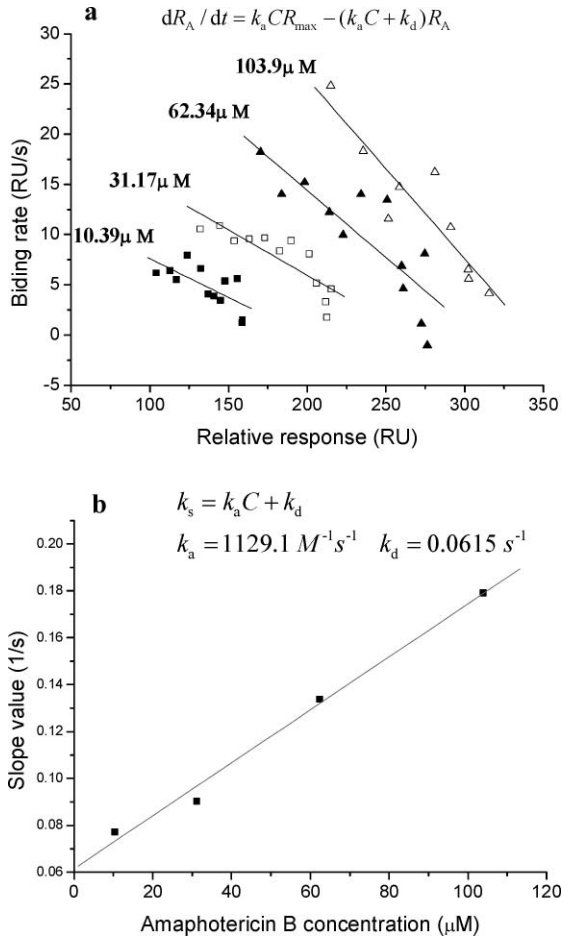

Fig. 6 (a) Plots of binding rates *vs.* relative response according to eqn (3); (b) analysis of rate constants in slope value *vs.* AmB concentration plot according to eqn (4); 25 μg mL^{-1} HSA was immobilized and the flow rate was 30 μL min^{-1}.

the simulated lines in Fig. 7(a) and 7(b). This phenomenon may be caused by the mass transport, steric hindrance, crowding and aggregation of high capacity surface.[31–33] Flow rate is also an important factor which may affect the binding process. To evaluate the effect of this factor, 5 μl min^{-1} was set as the flow rate on the high capacity surface. From Fig. 8, we can see that the equilibrium phase can not be obtained because the injected AmB solution can not be refreshed in time at a low flow rate during the injection process. Therefore a low capacity surface (5 μg mL^{-1}) and a high

Table 1 The kinetic parameters of the binding process[a]

Surface capacity/μg mL^{-1}	k_a/M^{-1} s^{-1}	k_d/s^{-1}	$K_A/\times 10^4$ M^{-1}	Average of $K_A/\times 10^4$ M^{-1}	R_{max} (RU)
25 (high)	1141	0.02172	5.253		
	910.9	0.01945	4.683	5.252 ± 0.568	410.0
	1229	0.02112	5.819		
5 (low)	1043	0.02615	3.989		
	961.7	0.02419	3.977	4.017 ± 0.060	264.7
	1374	0.03363	4.086		

[a] k_a—association rate constant; k_d—dissociation rate constant; K_A—equilibrium association constant; R_{max}—the total amount of binding sites of the immobilized ligand expressed as SPR response.

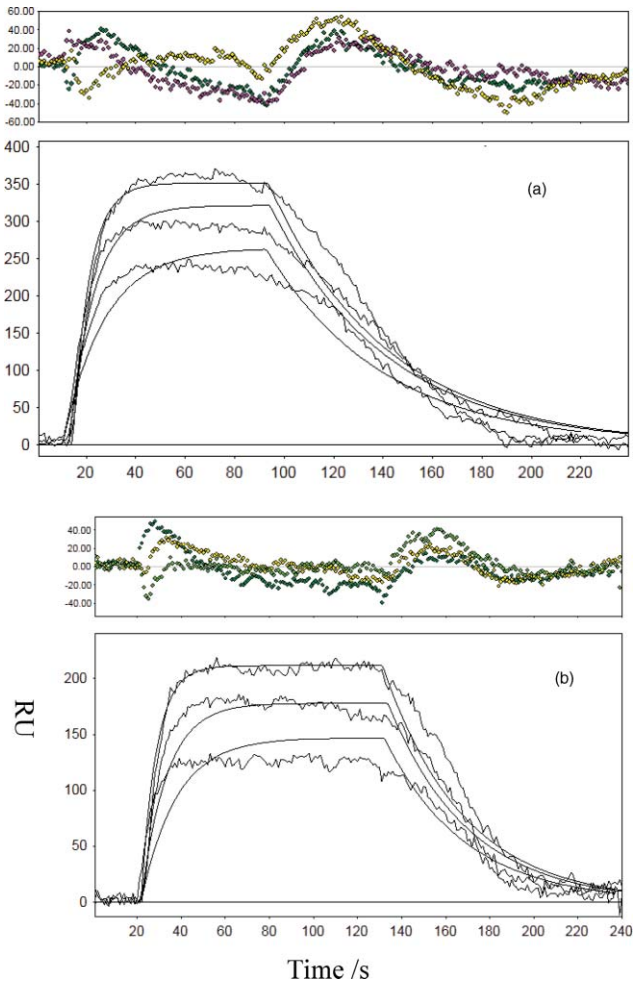

Fig. 7 (a) Sensorgrams of the binding between 25 μg mL^{-1}l HSA immobilized on the gold film and amphotericin B with the increasing concentration of 31.17 μM, 62.34 μM, 103.9 μM. The flow rate was 30 μl min^{-1} and the injection time was 100 s. The rough lines are the original data lines and the smooth lines are the simulated lines. (b) Sensorgrams of the binding between 5 μg mL^{-1} HSA immobilized on the gold film and amphotericin B with the increasing concentration of 31.17 μM, 51.95 μM, 103.9 μM. The flow rate was 50 μl min^{-1} and the injection time was 120 s. The rough lines are the original data lines and the smooth lines are the simulated lines.

flow rate (50 μl min^{-1}) were chosen as the optimal conditions, as shown in Fig. 7(b).

2.4 Experimental design of the fluorescence quenching results

Experimental designs are very important in chemometrics, since chemistry is essentially a field of science strongly dependent on chemical experiments. Experimental design is used to obtain a reaction product or chemical process with desirable characteristics in an efficient way. In this study, experimental design was used to optimize the fluorescence quenching process and obtain good results.

In this paper, excitation wavelength (W), excitation slit (E_x) and emission slit (E_m) were selected as the factors and the equilibrium association constant (K_{SV}) was selected as the response. For each factor, two levels were selected (Table 2).

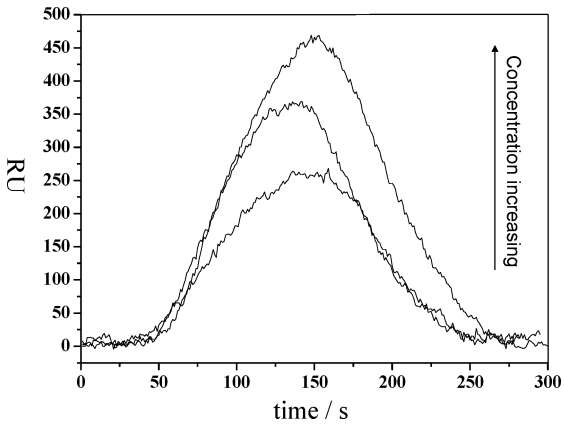

Fig. 8 Sensorgrams of the binding between 25 μg mL^{-1} HSA immobilized on the gold film and amphotericin B with increasing concentration (31.17 μM, 62.34 μM, 103.9 μM). The flow rate was 5 μl min^{-1} and the injection time was 100 s.

Table 2 The results of the 24 experimental runs

Factors			Results
W^a	$E_x{}^b$	$E_m{}^c$	K_{SV}/M^{-1}
+	−	−	25860.0 ± 1746.8
+	−	+	24996.2 ± 2188.4
+	+	−	27344.2 ± 1438.5
+	+	+	28443.5 ± 1344.8
−	−	−	31209.8 ± 1718.4
−	−	+	30533.3 ± 1474.6
−	+	−	36557.3 ± 1028.3
−	+	+	33842.4 ± 1353.7

[a] Excitation wavelength, W (−: 280 nm, +: 295 nm). [b] Excitation slit, E_x (−: 5 nm, +:10 nm) [c] Emission slit, E_m (−: 5 nm, + : 10 nm).

In this design, 8 different experiments should be performed with the combinations of the three factors. For each experiment three replicates were performed. Therefore 24 experimental runs should have to be done in a random order. Fig. 9 shows one of the fluorescence quenching processes of HSA titrated with AmB. The other fluorescence quenching experiments have a similar quenching process.

K_{SV} was calculated by the Stern–Volmer equation:

$$\frac{F_0}{F} = 1 + K_{SV}[Q]$$

where F_0 and F are the fluorescence intensities in the absence and presence of the quencher, [Q] is the concentration of the quencher, and K_{SV} is the Stern–Volmer quenching constant. Hence the above equation could be used to determine K_{SV} by linear regression of a plot of F_0/F *versus* [Q] (Fig. 10). The results (K_{SV}) are shown in Table 2.

Factor effect is a method normally used in experimental design. The main effect of a single factor and the interactive effect between the factors on the response were calculated.

Fig. 11 gives the normal plot of effects by plotting the cumulative probability (P) against the value of factor effect (X). P can be calculated using the following equation

$$P_i = 100 \times (i - 0.5)/T$$

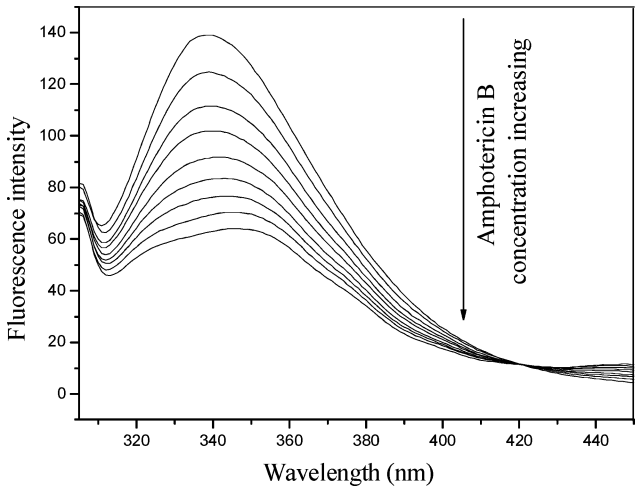

Fig. 9 Fluorescence emission spectra of 2×10^{-6}M HSA quenched by amphotericin B (0, 5, 10, 15, 20, 25, 30, 35, 40 μM). The excitation wavelength was 295 nm; the excitation slit and emission slit were set as 10 nm and 5 nm respectively.

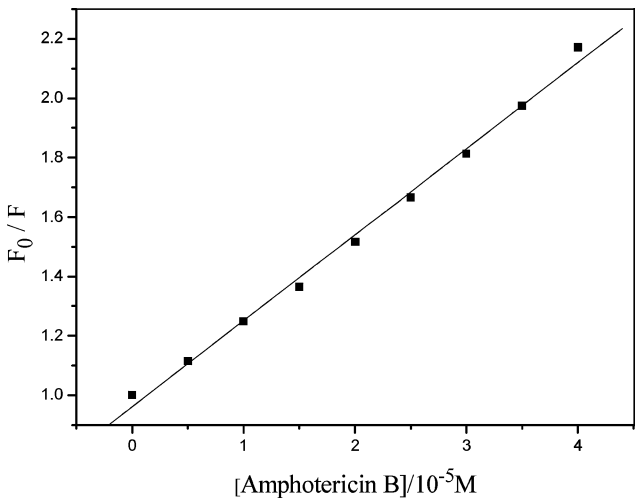

Fig. 10 Plot of F_0/F *versus* the concentration of amphotericin B. The excitation wavelength was 295 nm, the excitation slit and emission slit were set as 10 nm and 5 nm respectively. (Data are from Fig. 9).

where P_i is the expected probability of the i^{th} effect. T is the total number of effects ($T = 7$ in this paper) and i is the rank of the effect between 1 and T.

Plotting the cumulative probability (P) *vs.* effect provides an effective way to screen the factors. The technique works because most of the negligible effects will fall on a straight line. The effects which can not lie on a straight line with others are significant factors. In Fig. 11 there are obvious deviations between W (excitation wavelength), E_x (excitation slit) effects and the linear line formed from other effects. Therefore we can say that the excitation wavelength and excitation slit are two significant factors which can affect the results.

As shown in Table 2, the maximum K_{SV} value was obtained when the excitation wavelength was 280 nm, the excitation slit was 10 nm and the emission slit was 5 nm. This value was selected as the most reliable Stern–Volmer quenching constant which could

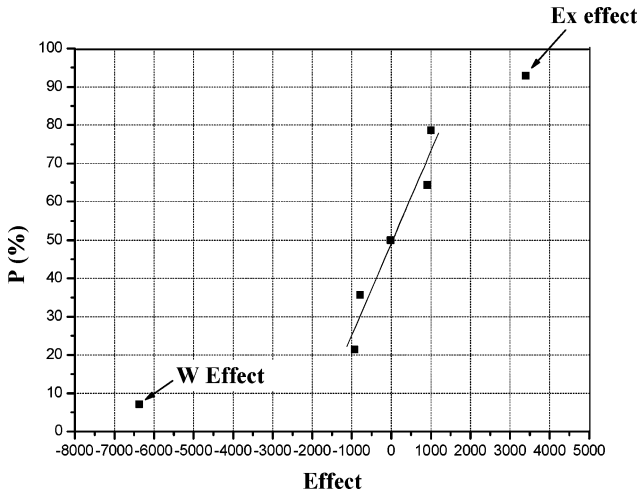

Fig. 11 Normal plots of cumulative probability (P) *vs.* effects.

be treated as the equilibrium association constant compared to the values obtained using the SPR method.

3. Experimental

3.1 Materials

Amphotericin B (Fig. 1) was purchased from Amesco. *N*-(3-dimethylaminopropyl)-*N*′-ethylcarbodiimide hydrochloride (EDC) was purchased from Fluka. *N*-hydroxysuccinimide (NHS) and 11-mercaptoundecanoic acid (11-MUA) was purchased from Aldrich. Ethanolamine and sodium acetate were purchased from Acros. Human Serum Albumin (HSA) was purchased from Sigma and was used without further purification. All the other starting materials were analytical grade. PBS (137 mM NaCl, 2.7 mM KCl, 10 mM $Na_2HPO_4 \cdot 12H_2O$, 2 mM KH_2PO_4, pH = 7.4) was used as the buffer solution in fluorescence and SPR experiments.

In the fluorescence experiments, HSA was dissolved in PBS to form a 2×10^{-6} M solution. In the SPR experiments HSA was dissolved in a 10 mM sodium acetate solution (pH = 5.0). PBS and sodium acetate solutions were filtered using 0.22 μm Millipore Express PES Membrane before used. Ethanolamine was dissolved in deionized water to form a 1 M solution and the pH was adjusted to 8.0 using hydrochloric acid. 11-MUA was dissolved in absolute ethanol to prepare a 5 mM solution.

3.2 SPR instrument

Fig. 12 shows the schematic diagram of the SPR. The instrument consists of a SPR monitor (parts 4, 5, 6), a flow injection system (parts 1, 2, 3), exchangeable sensors chips (part 7) and a data collection system (computer). More detailed information can be found in ref. 34. The shift in resonance angle is recorded as the signal. The unit for the SPR signal is the resonance unit (RU) where 1000 RU represents a shift in resonance angle of 0.1°.[9]

3.3 Gold film preparation

Fisher BK7 (catalog no. 12-540-A) glass slides were used as the glass substrates. First, the slides were heated in piranha solution (3 : 1 mixture of sulfuric acid and 30% hydrogen peroxide) at 80 °C for 30 min. After cooling, the glass slides were thoroughly cleaned

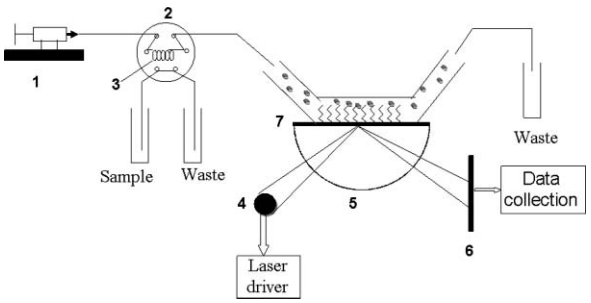

Fig. 12 A diagram of the SPR setup. 1. Syringe pump (KDS100, KD Scientific Inc. USA); 2. six port valve; 3. sample loop; 4. diode laser with a collimator and a focusing lens; 5. prism; 6. bi-cell photodetector; 7. glass slide coated with a thin Au film.

with water. Then the slides were sonicated in a 5 : 1 : 1 mixture of H_2O, NH_4OH and 30% H_2O_2. Before being coated with gold, the glass slides were dried with nitrogen.

A 50 nm gold film was deposited onto a 2 nm Cr adhesion layer using a Cressington 108 Automatic Sputter Coater combined with a Cressington High Resolution Thickness Monitor MTM-20 to monitor the thickness of the metal layer.

Each gold film was annealed in a hydrogen flame to reduce surface contamination and then the films were immersed in a 5 mM 11-MUA solution prepared in absolute ethanol for 24 h. Then the gold films were rinsed several times with ethanol and deionized water. After rinsing, the gold films were dried with pure N_2 gas stream. Then the gold film was ready to be placed on the SPR instrument.

3.4 Electrochemical measurements

Electrochemical measurements were carried out on a CHI830A electrochemical analyser (Shanghai, China). A three-electrode system was used in the measurements, with the bare gold film or 11-MUA modified gold film (immersed in 5 mM 11-MUA ethanol solution for 24 h) as the working electrode, a saturated calomel electrode (SCE) as the reference electrode and Pt as the counter electrode. All potentials given were referred to the SCE. Cyclic voltammograms of the bare and 11-MUA modified gold films were measured in two solutions: 0.1 M phosphate buffer solution (Na_2HPO_4, KH_2PO_4, pH = 7.0) and 1 mM $K_3Fe(CN)_6$ (0.1M KCl).

3.5 X-Ray photoelectron spectroscopy (XPS) measurements

XPS measurements were performed on the instrument of Kratos, XSAM800. The 11-MUA modified gold film was incised to form a small sized film, a bit smaller than 6 × 10 mm. Then it was placed on the instrument.

3.6 Immobilization of HSA

First, NHS–EDC (0.05 : 0.2 M) was injected to activate the carboxyl groups. Second, HSA (25 μg mL^{-1} or 5 μg mL^{-1}) was injected and immobilized on the surface because of the formation of 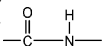 bond. The final immobilization levels were 11000 RU and 5000 RU respectively. Then, 1 M ethanolamine was injected to block the unreacted carboxyl groups. Finally, a 50 s pulse injection of 50 mM sodium hydroxide was injected to remove any noncovalently bound HSA.

3.7 Amphotericin B binding to HSA

AmB was prepared as a 1.039 mM stock solution in PBS. Immediately prior to analysis, amphotericin B was diluted with PBS to final concentration of 10.39 μM, 31.17 μM, 51.95 μM, 62.34 μM and 103.9 μM. Once a sample was injected into the flow system, the response was monitored until the signal returned to the baseline, which indicated that the amphotericin B was all removed from the surface. For the film on which 25 μg mL^{-1} HSA was immobilized, the flow rate was set as 30 μL min^{-1} and the injection lasted for 100 s. While for the film immobilized 5 μg mL^{-1} HSA the flow rate was set as 50 μL min^{-1} and the injection time was 120 s.

3.8 Data analysis

For fluorescence data, a 2^3 factorial design was used to find the most effective factor which may affect the fluorescence results.

ClampXP, a data analysis program designed to interpret the kinetics of binding reactions recorded on biosensors, was used to analyze the SPR data. This program can do global analysis of the data. Also, using this program, the data at different concentrations were screened and three concentrations were selected for the calculation of the kinetic parameters. For 25 μg mL^{-1} HSA, 31.17 μM, 62.34 μM and 103.9 μM were used. For 5 μg mL^{-1} HSA, 31.17 μM, 51.95 μM and 103.9 μM were used.

3.9 Fluorescence quenching measurements

All fluorescence spectra were recorded on a F-2500 spectrofluorimeter (Hitachi, Japan) with a 1 × 1 × 4 cm cell. The emission spectra in absence and presence of AmB were recorded at 305–450 nm. Human serum albumin samples were titrated with AmB by using trace syringes with the final concentration of AmB in the range of 0–4 × 10^{-5} M.

4. Conclusion

In this study, the equilibrium association constant K_A obtained from the SPR measurements is 4.017 × 10^4 M^{-1}, and the maximum equilibrium association constant K_{SV} obtained from the fluorescence measurements is 3.656 × 10^4 M^{-1}. It is obvious that K_{SV} is a little smaller than K_A, but they have the same magnitude. Fluorescence quenching, as a traditional and classical method, has been used to obtain the equilibrium association constants of this kind of interaction for many years. Therefore, we can say that the SPR method used in our research is suitable to study the drug–protein interaction because of the similar values of K_A and K_{SV}. In fact, the SPR method has been accepted as the most accurate technique to obtain the kinetic parameters of the macromolecular interactions.

The fluorescence quenching method is based on quenching of tryptophan residue when the excitation wavelength is set between 280 nm and 295 nm. That is to say the method focuses on the interaction between tryptophan and amphotericin B. When the fluorescence intensity decreases with the addition of amphotericin B, it is thought that the microenvironment of the tryptophan changed and the binding occurred between amphotericin B and

HSA. Therefore the fluorescence quenching method does not consider the interaction between amphotericin B and other sites on HSA. However, SPR is a kind of method based on the refractive index change of a solid surface. The entire signal caused by any interaction may be recorded but without considering the binding sites.

Therefore, the both methods can be used to detect drug–protein interactions. However, each method has its own advantage. To obtain an accurate association constant between the drug and serum albumins, the SPR method should be chosen; while to study the binding sites, the fluorescence method should be chosen.

Acknowledgements

We gratefully acknowledge financial support from the National Natural Science Foundation of China (30570015, 20621502); Natural Science Foundation of Hubei Province (2005ABC002); Science Research Foundation of Chinese Ministry of Education ([2006]8IRT0543), and the 863 program from the Chinese Ministry of Science and Technology (2007AA06Z407).

References

1 Xiao Min He and Daniel C. Carter, Atomic structure and chemistry of human serum albumin, *Nature*, 1992, **358**, 209–215.
2 Robert Arnell, Natalia Ferraz and Torgny Fornstedt, Analytical Characterization of Chiral Drug–Protein Interactions: Comparison between the Optical Biosensor (Surface Plasmon Resonance) Assay and the HPLC Perturbation Method, *Anal. Chem.*, 2006, **78**, 1682–1689.
3 Jennifer Sykora, Solomon Yilma, William C. Neely and Vitaly Vodyanoy, Amphotericin B and Cholesterol in Monolayers and Bilayers, *Langmuir*, 2003, **19**, 858–864.
4 Andreas Zumbuehl, Pasquale Stano, Dominik Heer, Peter Walde and Erick M. Carreira, Amphotericin B as a Potential Probe of the Physical State of Vesicle Membranes, *Org. Lett.*, 2004, **6**, 3683–3686.
5 Nobuaki Matsumori, Toshihiro Houdai and Michio Murata, Conformation and Position of Membrane-Bound Amphotericin B Deduced from NMR in SDS Micelles, *J. Org. Chem.*, 2007, **72**, 700–706.
6 M. Page Haynes, Parkson Lee-Gau Chong, Helen R. Buckley and Ronald A. Pieringer, Fluorescence Studies on the Molecular Action of Amphotericin B on Susceptible and Resistant Fungal Cells, *Biochemistry*, 1996, **35**, 7983–7992.
7 R. Seoane, J. Minones, O. Conde, M. Casas and E. Iribarnegaray, Interaction between Amphotericin B and Sterols in Monolayers. Mixed Films of Ergosterol-Amphotericin B, *Langmuir*, 1999, **15**, 3570–3573.
8 Jiri Homola and Sinclair S. Yee, *et al.*, Surface plasmon resonance sensors: review, *Sens. Actuators, B*, 1999, **54**, 3–15.
9 K. Nagata, H. Handa, *Real-Time Analysis of Biomolecular Interactions*, Springer-Verlag, New York, 2000.
10 Peter Schuck, Use of Surface Plasmon Resonance to probe the equilibrium and dynamic aspects of interactions between biological macromolecules, *Annu. Rev. Biophys. Biomol. Struct.*, 1997, **26**, 541–566.
11 Rebecca L. Rich and David G. Myszka, Survey of the 1999 surface plasmon resonance biosensor literature, *J. Mol. Recognit.*, 2000, **13**, 388–407.
12 Rebecca L. Rich and David G. Myszka, Survey of the 2000 surface plasmon resonance biosensor literature., *J. Mol. Recognit.*, 2001, **14**, 273–294.
13 Rebecca L. Rich and David G. Myszka, Survey of the 2001 surface plasmon resonance biosensor literature, *J. Mol. Recognit.*, 2002, **15**, 352–376.
14 Rebecca L. Rich and David G. Myszka, Survey of the 2002 surface plasmon resonance biosensor literature, *J. Mol. Recognit.*, 2003, **16**, 351–382.
15 Rebecca L. Rich and David G. Myszka, Survey of the 2003 surface plasmon resonance biosensor literature, *J. Mol. Recognit.*, 2005, **18**, 1–39.
16 Rebecca L. Rich and David G. Myszka, Survey of the 2004 surface plasmon resonance biosensor literature, *J. Mol. Recognit.*, 2005, **18**, 431–478.
17 Rebecca L. Rich and David G. Myszka, Survey of the 2005 surface plasmon resonance biosensor literature, *J. Mol. Recognit.*, 2006, **19**, 478–534.
18 Xia Liu, Daqian Song, Qinglin Zhang, Yuan Tian, Zhongying Liu and Hanqi Zhang, Characterization of drug-binding levels to serum albumin using a wavelength modulation surface plasmon resonance sensor, *Sens. Actuators, B*, 2006, **117**, 188–195.
19 Frank Schubert, Heiko Zettl, Wolfgang Hafner, Gerhard Krauss and Georg Krausch, Comparative Thermodynamic Analysis of DNA-Protein Interactions Using Surface Plasmon Resonance and Fluorescence Correlation Spectroscopy, *Biochemistry*, 2003, **42**, 10288–10294.
20 Huey Fang Teh, Wendy Y. X. Peh, Xiaodi Su and Jane S. Thomsen, Characterization of Protein-DNA Interactions Using Surface Plasmon Resonance Spectroscopy with Various Assay Schemes, *Biochemistry*, 2007, **46**, 2127–2135.
21 Anand Subramanian, Joseph Irudayaraj and Thomas Ryan, Mono and dithiol surfaces on surface plasmon resonance biosensors for detection of Staphylococcus aureus, *Sens. Actuators, B*, 2006, **114**, 192–198.
22 Konstantin E. Komolov, Ivan I. Senin, Pavel P. Philippov and Karl-Wilhelm Koch, Surface Plasmon Resonance Study of G Protein/Receptor Coupling in a Lipid Bilayer-Free System, *Anal. Chem.*, 2006, **78**, 1228–1234.
23 K. Scott Phillips, Thomas Wilkop, Jiing-Jong Wu, Rabih O. Al-Kaysi and Quan Cheng, Surface Plasmon Resonance Imaging Analysis of Protein-Receptor Binding in Supported Membrane Arrays on Gold Substrates with Calcinated Silicate Films, *J. Am. Chem. Soc.*, 2006, **128**, 9590–9591.
24 Jing Zhao, Aditi Das, Xiaoyu Zhang, George C. Schatz, Stephen G. Sligar and Richard P. Van Duyne, Resonance Surface Plasmon Spectroscopy: Low Molecular Weight Substrate Binding to Cytochrome P450, *J. Am. Chem. Soc.*, 2006, **128**, 11004–11005.
25 Tatsuro Endo, Kagan Kerman, Ha Minh Hiepa, Do-Kyun Kim, Yuji Yonezawa, Koichi Nakano, Naoki Nagatani and Eiichi Tamiya, Multiple Label-Free Detection of Antigen-Antibody Reaction Using Localized Surface Plasmon Resonance-Based Core-Shell Structured Nanoparticle Layer Nanochip, *Anal. Chem.*, 2006, **78**, 6465–6475.
26 J. R. Lakowicz, *Principles of Fluorescence Spectroscopy*, Kluwer Academic Publishers/Plenum Press, New York, 2nd edn, 1999.
27 Dilson Silva, Célia M. Cortez, Jayme Cunha-Bastos and Sonia R.W. Louro, *Toxicol. Lett.*, 2004, **147**, 53–61.
28 E. D. Morgan, *Chemometrics: Experimental Design*, Analytical Chemistry by Open Learning, John Wiley & Sons, London, 1991.
29 Caroline M. Whelan, Malcolm R. Smyth, Colin J. Barnes, Norman M. D. Brown and Colin A. Anderson, An XPS study of heterocyclic thiol self-assembly on Au (111), *Appl. Surf. Sci.*, 1998, **134**, 144–158.
30 L. Pasquali, F. Terzi, C. Zanardi, L. Pigani, R. Seeber, G. Paolicelli, S. M. Suturin, N. Mahne and S. Nannarone, Structure and properties of 1,4-benzenedimethanethiol films grown from solution on Au(111): An XPS and NEXAFS study, *Surf. Sci.*, 2007, **601**, 1419–1427.
31 Lin D. Roden and David G. Myszka, Global Analysis of a Macromolecular Interaction Measured on BIAcore, *Biochem. Biophys. Res. Commun.*, 1996, **225**, 1073–1077.
32 David G. Myszka, Improving biosensor analysis, *J. Mol. Recognit.*, 1999, **12**, 279–284.
33 Paula Gomes, Ernest Giralt and David Andreu, Direct single-step surface plasmon resonance analysis of interactions between small peptides and immobilized monoclonal antibodies, *J. Immunol. Methods*, 2000, **235**, 101–111.
34 Fayi Song, Feimeng Zhou, Jun Wang, Nongjian Tao, Jianqiao Lin, Robert L. Vellanoweth, Yvonne Morquecho and Janel Wheeler-Laidman, Detection of oligonucleotide hybridization at femtomolar level and sequence-specific gene analysis of the Arabidopsis thaliana leaf extract with an ultrasensitive surface plasmon resonance spectrometer, *Nucleic Acids Res.*, 2002, **30**, e72.